Biochemistry

Article

Cite This: Biochemistry 2017, 56, 5663-5670

pubs.acs.org/biochemistry

Active Site Metal Identity Alters Histone Deacetylase 8 Substrate Selectivity: A Potential Novel Regulatory Mechanism

Carol Ann Castaneda,[†] Jeffrey E. Lopez,[†,@] Caleb G. Joseph,[‡,#] Michael D. Scholle,[§,⊥] Milan Mrksich,[*,§] and Carol A. Fierke[*,‡,†,∥]

[†]Program in Chemical Biology, University of Michigan, Ann Arbor, Michigan 48109, United States

[‡]Department of Medicinal Chemistry, University of Michigan, Ann Arbor, Michigan 48109, United States

[§]Department of Chemistry and Department of Biomedical Engineering, Northwestern University, Evanston, Illinois 60208, United States

[∥]Department of Chemistry and Department of Biological Chemistry, University of Michigan, Ann Arbor, Michigan 48109, United States

ABSTRACT: Histone deacetylase 8 (HDAC8) is a well-characterized member of the class I acetyl-lysine deacetylase (HDAC) family. Previous work has shown that the efficiency of HDAC8-catalyzed deacetylation of a methylcoumarin peptide varies depending on the identity of the divalent metal ion in the HDAC8 active site. Here we demonstrate that both HDAC8 activity and substrate selectivity for a diverse range of peptide substrates depend on the identity of the active site metal ion. Varied deacetylase activities of Fe(II)- and Zn(II)-HDAC8 toward an array of peptide substrates were identified using self-assembled monolayers for matrix-assisted laser desorption ionization (SAMDI) mass spectrometry. Subsequently, the metal dependence of deacetylation of peptides of biological interest was measured using an *in vitro* peptide assay. While Fe(II)-HDAC8 is generally more active than Zn(II)-HDAC8, the Fe(II)/Zn(II) HDAC8 activity ratio varies widely (from 2 to 150) among the peptides tested. These data provide support for the hypothesis that HDAC8 may undergo metal switching *in vivo* that, in turn, may regulate its activity. However, future studies are needed to explore the identity of the metal ion bound to HDAC8 in cells under varied conditions.

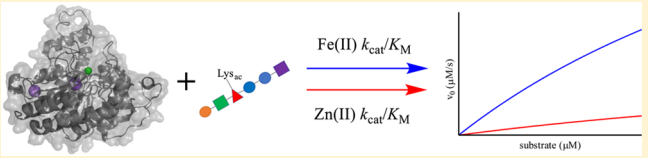

Protein lysine acetylation is an enzymatically reversible post-translational modification. Acetylation is catalyzed by 20 lysine acetyl transferases (KATs), and hydrolysis of the acetyl moiety is catalyzed by 18 acetyl-lysine deacetylases, including the metal-dependent histone deacetylases (HDACs) and the NAD(+)-dependent sirtuins (SIRTs). The balance of the enzymatic activities of HDACs and KATs regulates the acetylation state of the >3800 acetylated sites on thousands of proteins in the mammalian proteome involved in many cellular processes.[2,3] With such a modest number of enzymes catalyzing the same chemistry on thousands of substrates, it is important to understand the mechanisms by which the selectivity of the enzymes is regulated.[4,5] HDACs are medically relevant enzymes; aberrant HDAC activity is implicated in a number of disease states.[5] Elucidating the determinants of HDAC substrate specificity will inform the engineering of selectivity into novel therapeutics targeting these enzymes.

HDAC8 is a biochemically well-characterized metal-dependent HDAC. However, the protein substrates, cellular role, and regulation are still under investigation. This enzyme is expressed in both the nucleus and the cytoplasm, with the highest expression levels in smooth muscle cells.[6,7] Predicted HDAC8 substrates include the nuclear structural maintenance of chromosomes 3 (SMC3),[8] histone proteins,[9] and several cytosolic substrates such as estrogen-related receptor α (ERRα).[10,11] HDAC8 was originally described as a zinc-dependent enzyme because zinc is copurified with the enzyme, and this metal was visualized in the first HDAC8 crystal structure.[12,13] However, several metal ions activate the enzyme. The k_{cat}/K_M (catalytic efficiency) trend, measured using a short methylcoumarin peptide substrate, for metal-substituted HDAC8 is Co(II) > Fe(II) > Zn(II).[1] Furthermore, the inhibition constant, K_i, for the T-cell lymphoma drug suberoylanilide hydroxamic acid (SAHA) is different for each metal-substituted HDAC8. The trend of inhibition constants is the inverse of that of k_{cat}/K_M, with Co(II)-HDAC8 binding SAHA most tightly.[14] The fact that HDAC8 is activated by several divalent metal ions may suggest metal-dependent regulation of this enzyme *in vivo*.

Crystal structures of metal-substituted HDACs have not provided an explanation for the differential activation and inhibition. Structures of Fe(II)-, Co(II)-, and Zn(II)-HDAC8 bound to the hydroxamic acid (metal-chelating) inhibitor M344 demonstrate a common ligand coordination geometry for the three metal-substituted enzyme forms.[14] The inhibitor-bound structures are a snapshot and cannot show the conformational changes or dynamic interactions that may occur when the

Received: August 29, 2017
Revised: September 14, 2017
Published: September 22, 2017

DOI: 10.1021/acs.biochem.7b00851
Biochemistry 2017, 56, 5663−5670

substrate binds to the enzyme and that may impact the activity and selectivity of HDAC8. Additionally, it is possible that the bound hydroxamic acid stabilizes a common metal coordination state regardless of the metal ion.

Protein metalation in cells is complicated, and not yet well-understood for many enzymes, but it depends on both cellular availability and, in some cases, metallochaperones.[15] Either Zn(II)- or Fe(II)-HDAC8 is a candidate for the *in vivo* enzyme form based on cellular metal concentrations and the affinity of HDAC8 for each metal. Exchangeable Zn(II) is present at an estimated readily exchangeable concentration 10^5-fold lower than that of Fe(II),[16−20] but it has a 10^6-fold higher affinity for HDAC8.[1,14] Fe(II)-HDAC8 is sensitive to oxidation and is not activated by Fe(III); acetyl-lysine deacetylase activity in both bacterial and mammalian cell lysates is oxygen sensitive, suggesting the presence of Fe(II)-dependent activity.[1,21] Moreover, immunopurified HDAC8 overexpressed in HeLa tissue culture cells demonstrates oxygen sensitive activity, as well.[21] Taken together, the data to date suggest that iron may play a role in cellular HDAC8 activation and demonstrate the importance of determining which metal(s) activates and regulates HDAC8 *in vivo*.

Prompted by the difference in metal-dependent activity and the HDAC8 oxygen sensitivity, we further investigated the extent of the effect of metal ion identity on HDAC8 activity. Here we show, for the first time, that HDAC8 substrate selectivity depends on the identity of the metal ion at the active site; the selectivity toward peptide substrates changes in concert with the active site metal ion. This work suggests a new mechanism by which the specificity of HDAC8 may be regulated, with implications for cellular regulation of acetylation and deacetylase-targeting therapeutics.

METHODS

Metal free HEPES, NaCl, KCl, and NaOH were purchased from Sigma. TCEP was purchased from GoldBio. All other reagents were purchased from Fisher unless otherwise specified.

Recombinant HDAC8 Purification. HDAC8 was prepared using the following method, modified from ref 13. HDAC8-TEV-6His was transformed into BL21-DE3 Z-competent cells and grown in 2xYT medium supplemented with 100 μg/mL ampicillin at 37 °C until the OD_{600} reached 0.4−0.7. The temperature was decreased to 20 °C for 45−60 min, followed by induction with isopropyl β-D-1-thiogalactopyranoside (IPTG, 0.5 mM) and addition of $ZnSO_4$ (0.2 mM). Cells were harvested 15−16 h postinduction by centrifugation (4000*g* for 15−20 min at 4 °C) and resuspended in HDAC8 purification buffer [30 mM HEPES (pH 8), 150 mM NaCl, 1 mM imidazole, and 1 mM TCEP] supplemented with a complete protease inhibitor cocktail tablet (Roche). Cells were lysed using a microfluidizer (Microfluidics), followed by nucleic acid precipitation with polyethylenimine (pH 7.9) and centrifugation (27000*g* for 45 min at 4 °C). The supernatant containing HDAC8 was loaded onto a Ni^{2+}-charged chelating sepharose (GE Healthcare) gravity column and equilibrated with HDAC8 purification buffer. The column was washed with 20 mM imidazole purification buffer, and HDAC8 was eluted using a linear gradient (from 25 to 250 mM imidazole). The six-His tag was cleaved using a six-His-tagged TEV protease during an overnight dialysis against HDAC8 purification buffer without imidazole. A second stepwise elution from a Ni^{2+}-charged column was used to separate HDAC8 from TEV protease. HDAC8 was concentrated in 30K molecular weight cutoff Amicon Ultra centrifugal concentrators and dialyzed against metal chelating buffer A [25 mM MOPS (pH 7.5), 1 mM TCEP, 5 mM KCl, and 1 mM EDTA] followed by several serial dialyses against metal free buffer B [25 mM MOPS (pH 7.5), 1 mM TCEP, and 5 mM KCl]. For matrix-assisted desorption ionization (MALDI) deacetylation assays, a PD-10 desalting column (GE Healthcare) in either PD-10 buffer A [25 mM HEPES (pH 7.8), 150 mM NaCl, 3 mM KCl, and 1 mM TCEP] or PD-10 buffer B [25 mM MOPS (pH 7.5) and 1 mM TCEP] was used to remove residual EDTA. HDAC8 was aliquoted, flash-frozen in liquid nitrogen, and stored at −80 °C. The concentration was measured by the absorbance at 280 nm using an extinction coefficient of 52120 M^{-1} cm^{-1}, which was determined previously.[13] ICP-MS confirmed <10% Zn(II) was present in the final enzyme sample.

High-Throughput SAMDI Deacetylation Assays. Selectivity screens were performed using self-assembled monolayers for MALDI-TOF mass spectrometry (SAMDI). The SAMDI assays were performed as previously described.[16] Peptides of varying sequence were transferred to a SAMDI array plate containing 384 gold spots, each with a monolayer presenting a maleimide group at a density of 10% against a background of tri(ethylene glycol) groups. In this way, each peptide was immobilized to an individual spot through reaction of the thiol side chain of the terminal cysteine residue with a maleimide, while the glycol groups prevent nonspecific adsorption of proteins onto the monolayer. The peptide array was incubated with HDAC8, which had been reconstituted at a 1:1 enzyme:metal ion ratio, by dispensing 3 μL of a solution [0.5 μM enzyme, 25 mM Tris (pH 8.0), 147 mM NaCl, and 3 mM KCl] using a 12-channel pipet. Solutions were kept at 37 °C for 30 min, and then the reaction was stopped when the array plate was rinsed with ethanol.

Enzyme-Coupled Assay for Measuring Deacetylation of Non-Methylcoumarin Peptides. Peptides (Peptide 2.0 and/or Synthetic Biomolecules) were synthesized with an acetylated N-terminus and carboxyamide C-terminus. Zn(II)-HDAC8 and Fe(II)-HDAC8 were reconstituted as follows. Apo-HDAC8 (10 μM) was reconstituted with stoichiometric Zn(II) (Fluka) in peptide assay buffer [25 mM HEPES (pH 8), 137 mM NaCl, and 3 mM KCl] and incubated for 1 h on ice. For Fe(II)-HDAC8, apo-HDAC8 was equilibrated in an anaerobic glovebox (Coy Laboratory Products) for 1 h prior to reconstitution. Solid $FeCl_2$ (Sigma), L-(+)-ascorbic acid (Fluka), and peptide assay buffer were equilibrated in the anaerobic chamber at least overnight. Fe(II) (100 μM) in 5 mM ascorbate and assay buffer was prepared daily. Fe(II)-HDAC8 (10 μM) was reconstituted anaerobically with a 5-fold excess of Fe(II) in assay buffer and 2.5 mM ascorbate for 1 h in a 0−4 °C CoolBox (Biocision) and kept on ice until use. Assays with Fe(II)-HDAC8 were performed aerobically on ice within 2 h, the effective working time for ascorbic acid to preserve Fe(II)-HDAC8 activity.[22] The enzyme-coupled assay couples acetate production to the formation of NADH and was performed as described previously.[19] Fe(II)- and Zn(II)-HDAC8 and peptides in assay buffer were individually equilibrated at 30 °C for 15 min prior to initiation of the reaction. Reactions were initiated by the addition of enzyme (1 μM) to various concentrations of substrates (25−400 μM). Time points were quenched in 10% hydrochloric acid (HCl), flash-frozen in liquid nitrogen, and stored at −80 °C. Assay workup was performed as described previously.[19] Standards were prepared using acetic acid (Ricca Chemical Co.). After

DOI: 10.1021/acs.biochem.7b00851
Biochemistry 2017, 56, 5663−5670

samples had been thawed, time points were neutralized with 6% sodium bicarbonate ($NaHCO_3$), centrifuged (16000*g* for 1 min), and added to an equilibrated coupled enzyme solution in a 96-well plate (Corning). The fluorescence of the resulting NADH was measured (excitation at 340 nm, emission at 460 nm), and the initial rate was calculated from the time dependence of NADH production. The Michaelis−Menten (MM) equation or a line was fit to the concentration dependence of the initial rate to calculate kinetic parameters (k_{cat}, K_M, and k_{cat}/K_M).

Assay for Measuring Methylcoumarin-Labeled Peptides. Peptides containing a methylcoumarin-bound C-terminus were measured using the Fluor-de-Lys (FdL) assay (Enzo Life Sciences). Deacetylation of the substrates catalyzed by HDAC8 is followed by cleavage of the amide bond linking the C-terminal methylcoumarin to the peptide backbone catalyzed by trypsin, resulting in a shift in the fluorescence between the deacetylated product (excitation at 340 nm, emission at 450 nm) and the remaining substrate (excitation at 340 nm, emission at 380 nm). HDAC8 was reconstituted and equilibrated with either Fe(II) or Zn(II) as described previously. Reactions were initiated by the addition of enzyme (1 μM) to various concentrations of substrate (25−200 μM). Time points were quenched by the addition of trichostatin A (TSA) and trypsin developer. The initial rate was calculated from the time dependence of the changes in fluorescence with concentration determined from a standard curve. The MM equation or a line was fit to the concentration dependence of the initial rate to calculate kinetic parameters (k_{cat}, K_M, and k_{cat}/K_M).

RESULTS

SAMDI Deacetylation Assays. As an initial screen to evaluate the substrate selectivity of HDAC8 reconstituted with either Zn(II) or Fe(II), we used SAMDI to profile the reactivity of HDAC8 with a peptide array[23] and found that even with short (six-amino acid) peptides the substrate selectivity of HDAC8 is metal ion-dependent. The peptides were of the form GXK^{Ac}ZGC and were attached to a plate through reaction of the thiol side chain of the cysteine residue with a maleimide. The flanking residues X and Z were varied across 19 amino acids (all natural residues excluding cysteine). In side-by-side experiments, we reconstituted apo-HDAC8 with either Fe(II) or Zn(II) and reacted each of these enzyme forms with the peptide array. After incubation, the monolayers were analyzed by MALDI mass spectrometry using the SAMDI method to observe the masses of the substrate and product of the reaction. The extent of deacetylation for each peptide was determined by the ratio of the deacetylated peak area to the sum of the peak areas for the substrate and product.

Both Fe(II)- and Zn(II)-HDAC8 catalyze deacetylation of many of the acetylated peptides in the array (Figure 1A,B). For Zn(II)-HDAC8, 172 of the peptides resulted in no significant HDAC8 activity (<3% deacetylation), 72 peptides showed moderate HDAC8 activity (3−15% conversion), and 117 peptides showed high activity (>15% conversion). Similarly, Fe(II)-HDAC8 was inactive toward 139 of the peptides, moderately active toward 62 peptides, and highly active toward 160 peptides. These data are presented in heat maps for each Me(II)-HDAC8 (Figure 1A,B).

To quantify differences in the reactivity of the metal-substituted enzymes, we calculated the ratio of the Zn(II)-HDAC8 to Fe(II)-HDAC8 product conversion and generated a specificity heat map in which the peptides are binned into four categories: little preference (gray, 122 peptides), higher reactivity with Zn(II)-HDAC8 (red, 40 peptides), higher

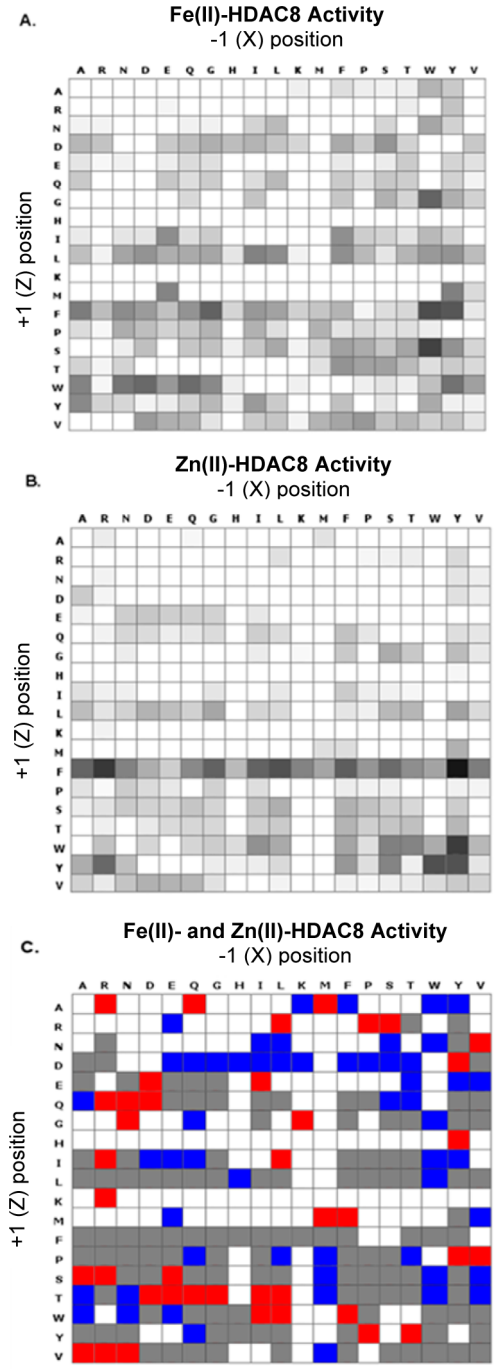

Figure 1. Heat maps visualizing HDAC8 activity and selectivity. The selectivity of (A) Fe(II)-bound and (B) Zn(II)-bound HDAC8 was determined by applying each metal-substituted enzyme form to an array of 361 peptides of the sequence GXK^{Ac}ZGC. The extent of deacetylation of each peptide is shown in gray scale on the heat maps. (C) A metal-dependent peptide selectivity heat map was generated by taking the ratio of Zn(II)-HDAC8 to Fe(II)-HDAC8 product conversion for each peptide. Peptides with a >7-fold preference for Zn(II)-HDAC8 are colored red, and Fe(II)-selective peptides are colored blue. Peptides that were deacetylated similarly by both enzyme forms are colored gray, and peptides that were not deacetylated (<3%) by either enzyme form are colored white.

DOI: 10.1021/acs.biochem.7b00851
Biochemistry 2017, 56, 5663−5670

Table 1. Fe(II)-HDAC8/Zn(II)-HDAC8 Reactivity Ratios for Deacetylation of Various Peptide Substrates[a]

protein	sequence	Fe(II) k_{cat}/K_M (M^{-1} s^{-1})	Zn(II) k_{cat}/K_M (M^{-1} s^{-1})	Fe(II)/Zn(II) ratio
H3K9 13-mer	TKQTARK(ac)STGGKA	290 ± 20	50 ± 5	6 ± 1
La-related protein 1	LGK(ac)FRR	1080 ± 180	7 ± 1	154 ± 33
SMC3 9-mer	RVIGAKK(ac)DQ	240 ± 80	14 ± 2	17 ± 6
SMC3 10-mer	RVIGAKK(ac)DQY	220 ± 40	36 ± 2	6 ± 1
CREB94	CKDLK(ac)RLFS	8 ± 0.5	2 ± 0.2	4 ± 0.5
THRAP3	LGDGK(ac)MKS	20 ± 8	10 ± 1	2 ± 0.8
CSRP2BP	STPVK(ac)FISR	660 ± 120	40 ± 11	17 ± 5
HDAC8 FdL	RHK(ac)K(ac)-coumarin	2300 ± 160[b]	800 ± 50[b]	3 ± 0.2[b]
SIRT1 FdL	RHKK(ac)-coumarin	6150 ± 870	460 ± 35	13 ± 2
Boc-K(ac)-FdL	Boc-K(ac)-coumarin	975 ± 120	255 ± 25	4 ± 0.6

[a]Metal selectivity and reactivity varied significantly with both the identity of the active site divalent metal ion and the residues at positions +1 and −1 of the acetyl-lysine. [b]Data for the HDAC8 Fluor-de-Lys (FdL) peptide were taken from ref 1.

reactivity with Fe(II)-HDAC8 (blue, 54 peptides), and little reactivity with HDAC8 (white, 145 peptides) (Figure 1C). This heat map demonstrates that the substrate selectivity of HDAC8 depends on the identity of the active site metal ion. In the screen, approximately 15% of the peptides were better substrates for Fe(II)-HDAC8, 11% were better substrates for Zn(II)-HDAC8, 34% of the peptides had comparable reactivity with both enzyme forms, and 40% of the peptides resulted in negligible deacetylation for at least one form of the enzyme.

In addition to differences in selectivity based on the active site metal ion, the arrays suggest general peptide sequence selectivity trends for HDAC8. For example, both HDAC8 metalloforms display a preference for peptides containing an aromatic side chain (F, W, or Y) on the C-terminal side of the acetyl-lysine residue, while methionine in the Z position was largely unfavorable to both enzyme forms.

Kinetic Assays Quantify Metal-Dependent Substrate Selectivity for Fe(II)- and Zn(II)-HDAC8. To further test the dependence of substrate selectivity on the identity of the active site metal ion, we next probed metal-dependent selectivity using *in vitro* kinetic assays in solution. Concurrent work to identify HDAC substrates has suggested interesting putative protein substrates, and we selected peptides from these proteins to enhance the biological relevance of the results. We assayed deacetylation of peptides (listed in Table 1) taken from acetylated proteins that have been proposed as *in vivo* substrates of HDAC8 using proteomic and computational methods.[24,25] The peptide length was varied to enhance solubility.

Deacetylation was quantified using an acetate−NADH coupled assay that measures the conversion of acetate product to NADH by fluorescence.[26,27] The quenched assay was performed using Zn(II)- or Fe(II)-HDAC8 under multiple-turnover conditions. The dependence of the initial rates of peptide deacetylation on the peptide concentration was used to calculate k_{cat}/K_M values (see Figure 2). We also measured the reactivity and metal selectivity of several commercially available coumarin-labeled peptides using changes in fluorescence upon deacetylation.

The catalytic efficiency for deacetylation of these peptides ranged from 2 to 800 M^{-1} s^{-1} for Zn(II)-HDAC8 and from 8 to 6000 M^{-1} s^{-1} for Fe(II)-HDAC8. The Fe(II)-HDAC8 enzyme was faster for all of the peptides tested in solution. The k_{cat}/K_M values varied widely for the two metal enzyme forms, as predicted by the HDAC8 selectivity in the initial screen. The Fe(II)- to Zn(II)-HDAC8 ratio of the k_{cat}/K_M values ranged from 2 to 154 (Figure 3 and Table 1). Variations in the metal-dependent activity (ratios of 3−13) are also observed for the commercially available coumarin-labeled peptides, despite the higher values of k_{cat}/K_M. In general, an increase in the value of k_{cat}/K_M for Fe(II)-HDAC8 correlates with an increase in the Fe(II)/Zn(II) selectivity ratio.

The lack of peptides with higher k_{cat}/K_M values for Zn(II)-HDAC8 than for Fe(II)-HDAC8 is a major difference between the SAMDI screen and the solution measurements. This

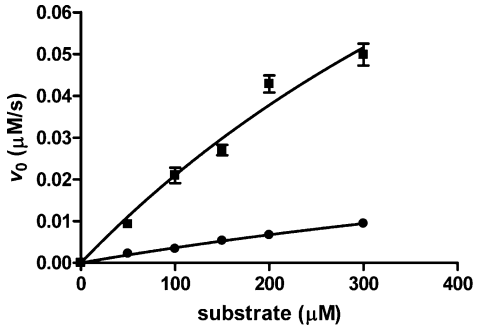

Figure 2. Representative peptide assay data. The dependence of the initial rate on substrate concentration for Fe(II)-HDAC8-catalyzed (■) and Zn(II)-HDAC8-catalyzed (●) deacetylation of the SMC3 10-mer peptide measured using the acetate assay. A hyperbola was fit to the data to calculate the Michaelis−Menten parameters.

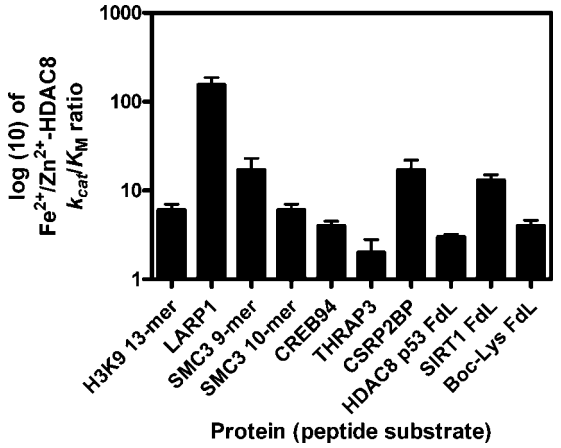

Figure 3. Fe(II)/Zn(II) reactivity ratios of various peptide substrates with HDAC8. Metal reactivity and selectivity varied significantly with the sequence of the peptide. Commercially available methylcoumarin-bound substrates were used as controls. HDAC8 p53 FdL data are reported in ref 1.

DOI: 10.1021/acs.biochem.7b00851
Biochemistry 2017, 56, 5663−5670

difference likely reflects alterations in the peptide structures and the assay conditions. First, the Fe(II)-HDAC8 activity in the SAMDI assay may be underreported as the enzyme was reconstituted with stoichiometric iron and was thus likely not saturated with Fe(II). Additionally, the SAMDI screen uses maleimide-modified peptides that are attached to a PEG-derivatized gold surface compared to the solution conditions of the peptide assays, and the SAMDI screen may measure values for k_{cat} rather than k_{cat}/K_M. Nonetheless, both assay methods clearly demonstrate that the Fe(II)/Zn(II) selectivity ratio varies significantly for different peptides.

DISCUSSION

Our in-solution peptide assays provide insight into several determinants of HDAC8 selectivity. First, while we did not set out to analyze the role of peptide length, our data suggest that this is not a primary determinant of selectivity, consistent with previous work.[28] The peptide with the highest Fe(II)/Zn(II) specificity ratio was six amino acids long, while peptides with ratios between 2 and 20 were eight or nine amino acids long.

Second, these data suggest that the peptide sequence is an important determinant of metal-dependent selectivity. For example, the two SMC3 peptides differ only in the presence or absence of a tyrosine at position +3, which leads to a significant difference in metal-dependent selectivity (17 ± 6 for the 9-mer and 6 ± 1 for the 10-mer). In this case, the change in the ratio results from a 2.5-fold decrease in the Zn(II)-dependent activity upon removal of the +3 Tyr residue. However, an aromatic side chain at position +3 is not sufficient to lead to high catalytic activity or a large Fe(II)/Zn(II) activity ratio. CREB94 has a Phe at position +3 but is a poor substrate for both metal-bound HDAC8 forms. The activities of Zn(II)-HDAC8 and Fe(II)-HDAC8 toward the CREB94 peptide are ∼2 and ∼8 M^{-1} s^{-1}, respectively, making the selectivity ratio ∼4.

The SAMDI screen predicts that HDAC8 has selectivity for an aromatic side chain at position +1, consistent with previous data.[23] Consistent with this, both of the peptides containing a Phe side chain at position +1 (La-related protein 1 and CSRP2BP) have the highest k_{cat}/K_M values for Fe(II)-HDAC8 and are both Fe(II)-selective peptides with Fe(II)/Zn(II) ratios of 154 and 17, respectively (Table 1). These two peptides share the following sequences: +1 Phe, −3 aliphatic, and +3/4 arginine. Nonetheless, the remaining alterations in sequence lead to the almost 10-fold difference in the Fe(II)/Zn(II) ratio. This alteration is due to an almost 2-fold decrease in activity of Fe(II)-HDAC8 toward CSRP2BP compared to La-related protein 1 combined with a 5-fold increase in the Zn(II)-HDAC8 activity toward deacetylation of CSRP2BP compared to La-related protein 1.

We attempted to predict the metal selectivity solely on the basis of the +1 (Z) and −1 (X) positions using the data from the SAMDI screen. This was successful for the two SMC3 peptides (X = K, and Z = D), predicting peptides that would react more rapidly with Fe(II)-HDAC8. However, the predictions for the other peptides were incorrect. The H3K9- and CREB-derived peptides were predicted as zinc-selective substrates; however, our kinetic analysis shows that these peptides react more rapidly with Fe(II)-HDAC8. Finally, the SAMDI screen suggests that peptides containing the +1 (Z) and −1 (X) amino acids observed in the THRAP3- and CSRP2BP-derived peptides should be inactive. This lack of correlation between the predictions from the SAMDI screen and the peptide kinetic data demonstrate that although the amino acids at positions +1 and −1 contribute to reactivity and metal-dependent selectivity, the residues at the other sites in the sequence are also important determinants of HDAC8 selectivity. Consistent with this, previous studies investigating the correlation between peptide sequence and HDAC8 activity using kinetic and computational studies have demonstrated that the three amino acids on both sides of the acetyl-lysine contribute to reactivity.[25,23] These data in our current work highlight the nuance of HDAC8 peptide sequence selectivity and demonstrate the complexity that the metal ion identity adds to substrate recognition.

Regulation of HDAC8 Activity by Metal Switching. The data presented here reveal novel insights into HDAC8 substrate selectivity and highlight the importance of addressing HDAC8 metal selectivity in both *in vitro* and *in vivo* studies, a facet of HDAC biochemistry that has been neglected. The activity data demonstrate that Fe(II)-HDAC8 catalyzes deacetylation of peptides at a rate comparable to or faster than that of Zn(II)-HDAC8. Although both protein structure and long-range HDAC8−substrate interactions contribute to substrate selectivity,[28,29] peptides mimic short-range substrate interactions[22] and are a useful predictor of possible cellular substrates. Thus, these peptide data suggest that either metal-bound form of HDAC8 could be a relevant *in vivo* deacetylase and that manipulating the metal-substituted HDAC8 identity in the cell could alter the pool of recognized substrates and thereby influence downstream cellular effects.

We showed previously that Fe(II)-HDAC8 had a k_{cat}/K_M value higher than that of Zn(II)-HDAC8 for the one commercial peptide tested.[1] Here we broaden the scope of peptide substrates and show that even among short 6-mer peptides, which interact with only the active site and substrate binding surface directly near the active site, there are significant differences in selectivity based on the identity of the metal ion. If the Fe(II)/Zn(II) activity ratio were constant, this would suggest intrinsic differences in the reactivity of the active site metal ion. However, the peptide-dependent variation in the Fe(II)/Zn(II) activity ratio suggests a more complicated mechanism of regulation involving both metals. In this case, variation of the active site metal ion alters both HDAC8 reactivity and selectivity. The structural basis for the metal-dependent substrate selectivity is unclear. Crystal structures of HDAC8 with bound ligands indicate that the substrate binding site is primarily composed of flexible loops that accommodate a range of substrates but also influence the enzyme's selectivity.[10,14,30−35] Furthermore, the residues that coordinate the active site metal ion (His180, Asp267, and Asp178) are positioned by these loops.[14] The intrinsic properties of the metal ion, including Lewis acidity and size, could influence the structure and dynamics of the loop regions and alter the binding interface presented to substrates. Additionally, altering the active site metal ion coordination is expected to propagate structural changes to the peptide binding site via the residues in the hydrophobic shell around the metal ligands.[36] However, alterations in the geometry of the metal polyhedron have not yet been observed; structures of Fe(II)-, Co(II)-, and Zn(II)-HDAC8 bound to the hydroxamic acid inhibitor M344 demonstrate a common ligand coordination geometry for the three metal-substituted enzyme forms.[14] The bound hydroxamic acid may stabilize the metal coordination geometry in the active site of HDAC8.

These results suggest that metal-dependent selectivity of HDAC8 may be important for regulating deacetylation in the

DOI: 10.1021/acs.biochem.7b00851
Biochemistry 2017, 56, 5663−5670

cell. The readily exchangeable concentrations of Zn(II) and Fe(II) in cells are estimated to be in the pico- and micromolar ranges, respectively, under normal conditions.[16−20] Therefore, HDAC8 could bind either Zn(II) or Fe(II) in cells despite the 10^6-fold higher affinity for Zn(II).[1,14] Furthermore, the relative concentrations of readily exchangeable Zn(II) and Fe(II) increase and decrease depending on the cellular context, suggesting the possibility of metal switching in response to cellular conditions.[37,38] Zn(II) concentrations can change by several orders of magnitude, from picomolar to nanomolar levels.[39] For example, cellular zinc is generally tightly buffered, but the concentration of exchangeable Zn(II) increases under redox stress as protein thiol groups that coordinate zinc are oxidized, releasing Zn(II).[39,40] The dependence of Fe(II) concentration on the redox state of the cell is unclear, although it is reasonable to assume that it might decrease under oxidative stress.[41]

Metal-dependent substrate selectivity and inhibitor selectivity have been observed in bacterial methionine aminopeptidases, as well as other enzymes. *Trypanosoma brucei* methionine aminopeptidase 1, while likely a zinc enzyme *in vivo*, is activated by multiple metal ions [Co(II), Zn(II), Ni(II), Mn(II), and Fe(II)] and displays metal-dependent substrate selectivity for short peptide substrates.[42] *Escherichia coli* methionine aminopeptidase demonstrates metal-dependent inhibitor selectivity [Fe(II), Co(II), and Mn(II)].[43] *Klebsiella oxytoca* acireductone dioxygenase is an example of a known cambialistic enzyme; if Fe(II) is bound, it catalyzes one reaction, and if Ni(II) or Co(II) is bound, it catalyzes a different chemical reaction.[44] The metal-dependent bacterial deacetylase LpxC from *E. coli* has been shown to bind either Zn(II) or Fe(II) based on the relative abundance of these metals in the cell.[45] In this case, Fe(II)-LpxC has an activity ~8-fold higher than that of the zinc-bound enzyme. We would expect a similar model for metal-dependent HDACs; Fe(II)-HDAC8 (K_D = 0.2−1 μM)[14,46] and/or apo-HDAC8 may exist when the Zn(II) concentration is low. However, with an increase in the exchangeable Zn(II) concentration, HDAC8 could exchange the active site metal ion to form Zn(II)-HDAC,[14,46] maintaining active HDAC8 but altering the activity level and substrate selectivity.

The trend of greater catalytic efficiency for the iron-bound enzyme among more physiological peptides is consistent with the hypothesis that HDAC8 is activated, at least in part, by Fe(II) in the cell. Interestingly, Fe(II)-HDAC8 activity toward these peptides shows a correlation with the Fe/Zn specificity ratio. It is possible that a high ratio of iron to zinc activity may be indicative of HDAC8 substrates *in vivo*. This is supported by the fact that the three highest Fe(II)/Zn(II) ratios correspond to proteins recently identified as potential HDAC8 substrates in a proteomics screen.[24] Conversely, despite *in vitro* activity, evidence suggesting that histones may not be principal targets of HDAC8 *in vivo* is beginning to accumulate,[24,47,48] and this is consistent with the H3K9 13-mer peptide having an Fe(II)/Zn(II) ratio of <10.

This study is the first to demonstrate that the peptide sequence selectivity of HDAC8 varies with the identity of the active site metal ion. The SAMDI peptide screen enabled a broad survey of enzyme selectivity, and the enzyme assays in solution demonstrate varied Fe/Zn selectivities toward substrates that are likely physiologically relevant. *In vivo* evidence consistent with the hypothesis of metal switching regulation is still needed; however, the data presented here are consistent with the possibility that a change in cellular conditions that alter metal ion concentrations is coupled to modulation of deacetylation of target proteins by dictating the identity of the active site metal ion.

AUTHOR INFORMATION

Corresponding Authors

*E-mail: fierke@umich.edu.

*E-mail: milan.mrksich@northwestern.edu.

ORCID

Jeffrey E. Lopez: 0000-0002-5329-0043

Milan Mrksich: 0000-0002-4964-796X

Present Addresses

⊥M.D.S.: SAMDI Tech, Inc., 3440 S. Dearborn St., Suite 220S. Chicago, IL 60616.

#C.G.J.: Abbott Dept. 04ZU, Bldg. AP8B, 100 Abbott Park Rd., Abbott Park, IL 60064-3500.

@J.E.L.: Chemical Biology Laboratory, National Cancer Institute, 376 Boyles St., Bldg 376, Frederick, MD 21702.

Author Contributions

C.A.C. and J.E.L. are co-first authors.

Funding

This work was funded by National Institutes of Health (NIH) Grants 5-R01-GM-040602 (C.A.F.) and F31-GM-116619 (J.E.L.), University of Michigan Chemistry-Biology Interface (CBI) training program NIH Grant 5T32GM008597 (C.A.C.), and the Rackham Graduate School (C.A.C. and J.E.L.). SAMDI screens were funded by the NTU-NU Institute for Nano-Medicine located at the International Institute for Nano-technology, Northwestern University, and the Nanyang Technological University, Singapore (Agreement 10/20/14).

Notes

The authors declare no competing financial interest.

REFERENCES

(1) Gantt, S. L., Gattis, S. G., and Fierke, C. A. (2006) Catalytic activity and inhibition of human histone deacetylase 8 is dependent on the identity of the active site metal ion. *Biochemistry 45* (19), 6170−8.

(2) Norris, K. L., Lee, J.-Y., and Yao, T. P. (2009) Acetylation Goes Global: The Emergence of Acetylation Biology. *Sci. Signaling 2* (97), pe76.

(3) Khoury, G. A., Baliban, R. C., and Floudas, C. A. (2011) Proteome-wide post-translational modification statistics: frequency analysis and curation of the swiss-prot database. *Sci. Rep. 1*, 90.

(4) Smith, K. T., and Workman, J. L. (2009) Introducing the acetylome. *Nat. Biotechnol. 27* (10), 917−9.

(5) Haberland, M., Montgomery, R. L., and Olson, E. N. (2009) The many roles of histone deacetylases in development and physiology: implications for disease and therapy. *Nat. Rev. Genet. 10* (1), 32−42.

(6) Waltregny, D., de Leval, L., Glénisson, W., Ly Tran, S., North, B. J., Bellahcène, A., Weidle, U., Verdin, E., and Castronovo, V. (2004) Expression of Histone Deacetylase 8, a Class I Histone Deacetylase, Is Restricted to Cells Showing Smooth Muscle Differentiation in Normal Human Tissues. *Am. J. Pathol. 165* (2), 553−564.

(7) Hu, E., Chen, Z., Fredrickson, T., Zhu, Y., Kirkpatrick, R., Zhang, G. F., Johanson, K., Sung, C. M., Liu, R., and Winkler, J. (2000) Cloning and characterization of a novel human class I histone deacetylase that functions as a transcription repressor. *J. Biol. Chem. 275* (20), 15254−64.

(8) Deardorff, M. A., Kaur, M., Yaeger, D., Rampuria, A., Korolev, S., Pie, J., Gil-Rodríguez, C., Arnedo, M., Loeys, B., Kline, A. D., Wilson, M., Lillquist, K., Siu, V., Ramos, F. J., Musio, A., Jackson, L. S., Dorsett, D., and Krantz, I. D. (2007) Mutations in Cohesin Complex Members SMC3 and SMC1A Cause a Mild Variant of Cornelia de Lange

DOI: 10.1021/acs.biochem.7b00851
Biochemistry 2017, 56, 5663−5670

Syndrome with Predominant Mental Retardation. *Am. J. Hum. Genet. 80* (3), 485−494.
(9) Buggy, J. J., Sideris, M. L., Mak, P., Lorimer, D. D., McIntosh, B., and Clark, J. M. (2000) Cloning and characterization of a novel human histone deacetylase, HDAC8. *Biochem. J. 350* (Part 1), 199−205.
(10) Wolfson, N. A., Pitcairn, C. A., and Fierke, C. A. (2013) HDAC8 substrates: Histones and beyond. *Biopolymers 99* (2), 112−126.
(11) Wilson, B. J., Tremblay, A. M., Deblois, G., Sylvain-Drolet, G., and Giguere, V. (2010) An acetylation switch modulates the transcriptional activity of estrogen-related receptor alpha. *Mol. Endocrinol. 24* (7), 1349−58.
(12) Finnin, M. S., Donigian, J. R., Cohen, A., Richon, V. M., Rifkind, R. A., Marks, P. A., Breslow, R., and Pavletich, N. P. (1999) Structures of a histone deacetylase homologue bound to the TSA and SAHA inhibitors. *Nature 401* (6749), 188−193.
(13) Vannini, A., Volpari, C., Filocamo, G., Casavola, E. C., Brunetti, M., Renzoni, D., Chakravarty, P., Paolini, C., De Francesco, R., Gallinari, P., Steinkühler, C., and Di Marco, S. (2004) Crystal structure of a eukaryotic zinc-dependent histone deacetylase, human HDAC8, complexed with a hydroxamic acid inhibitor. *Proc. Natl. Acad. Sci. U. S. A. 101* (42), 15064−15069.
(14) Dowling, D. P., Gattis, S. G., Fierke, C. A., and Christianson, D. W. (2010) Structures of metal-substituted human histone deacetylase 8 provide mechanistic inferences on biological function. *Biochemistry 49* (24), 5048−56.
(15) Foster, A. W., Osman, D., and Robinson, N. J. (2014) Metal preferences and metallation. *J. Biol. Chem. 289* (41), 28095−103.
(16) Bozym, R. A., Thompson, R. B., Stoddard, A. K., and Fierke, C. A. (2006) Measuring picomolar intracellular exchangeable zinc in PC-12 cells using a ratiometric fluorescence biosensor. *ACS Chem. Biol. 1* (2), 103−11.
(17) Vinkenborg, J. L., Nicolson, T. J., Bellomo, E. A., Koay, M. S., Rutter, G. A., and Merkx, M. (2009) Genetically encoded FRET sensors to monitor intracellular Zn2+ homeostasis. *Nat. Methods 6* (10), 737−40.
(18) MacKenzie, E. L., Iwasaki, K., and Tsuji, Y. (2008) Intracellular iron transport and storage: from molecular mechanisms to health implications. *Antioxid. Redox Signaling 10* (6), 997−1030.
(19) Qin, Y., Dittmer, P. J., Park, J. G., Jansen, K. B., and Palmer, A. E. (2011) Measuring steady-state and dynamic endoplasmic reticulum and Golgi Zn2+ with genetically encoded sensors. *Proc. Natl. Acad. Sci. U. S. A. 108* (18), 7351−6.
(20) Epsztejn, S., Kakhlon, O., Glickstein, H., Breuer, W., and Cabantchik, I. (1997) Fluorescence analysis of the labile iron pool of mammalian cells. *Anal. Biochem. 248* (1), 31−40.
(21) Gattis, S. G. (2010) Mechanism and metal specificity of zinc-depdendent deacetylases. Ph.D. Dissertation, University of Michigan, Ann Arbor, MI.
(22) Kim, B. C. (2014) Probing the determinants of the molecular recognition in metal-dependent deacetylase. Ph.D. Dissertation, University of Michigan, Ann Arbor, MI.
(23) Gurard-Levin, Z. A., Kim, J., and Mrksich, M. (2009) Combining mass spectrometry and peptide arrays to profile the specificities of histone deacetylases. *ChemBioChem 10* (13), 2159−61.
(24) Olson, D. E., Udeshi, N. D., Wolfson, N. A., Pitcairn, C. A., Sullivan, E. D., Jaffe, J. D., Svinkina, T., Natoli, T., Lu, X., Paulk, J., McCarren, P., Wagner, F. F., Barker, D., Howe, E., Lazzaro, F., Gale, J. P., Zhang, Y.-L., Subramanian, A., Fierke, C. A., Carr, S. A., and Holson, E. B. (2014) An unbiased approach to identify endogenous substrates of "histone" deacetylase 8. *ACS Chem. Biol. 9* (10), 2210−6.
(25) Alam, N., Zimmerman, L., Wolfson, N. A., Joseph, C. G., Fierke, C. A., and Schueler-Furman, O. (2016) Structure-Based Identification of HDAC8 Non-histone Substrates. *Structure 24* (3), 458−468.
(26) Wolfson, N. A., Pitcairn, C. A., Sullivan, E. D., Joseph, C. G., and Fierke, C. A. (2014) An enzyme-coupled assay measuring acetate production for profiling histone deacetylase specificity. *Anal. Biochem. 456* (0), 61−69.
(27) Baumann, M., Stürmer, R., and Bornscheuer, U. T. (2001) A High-Throughput-Screening Method for the Identification of Active and Enantioselective Hydrolases. *Angew. Chem., Int. Ed. 40* (22), 4201−4204.
(28) Castaneda, C. A., Wolfson, N. A., Leng, K. R., Kuo, Y.-M., Leng, K. R., Andrews, A. J., and Fierke, C. A. (2017) Histone deacetylase 8 substrate specificity for full-length histone substrates is determined by long- and short-range interactions. Manuscript submitted for publication.
(29) Gurard-Levin, Z. A., and Mrksich, M. (2008) The Activity of HDAC8 Depends on Local and Distal Sequences of Its Peptide Substrates. *Biochemistry 47*, 6242−6250.
(30) Dowling, D. P., Gantt, S. L., Gattis, S. G., Fierke, C. A., and Christianson, D. W. (2008) Structural studies of human histone deacetylase 8 and its site-specific variants complexed with substrate and inhibitors. *Biochemistry 47* (51), 13554−63.
(31) Vannini, A., Volpari, C., Gallinari, P., Jones, P., Mattu, M., Carfi, A., De Francesco, R., Steinkuhler, C., and Di Marco, S. (2007) Substrate binding to histone deacetylases as shown by the crystal structure of the HDAC8-substrate complex. *EMBO Rep. 8* (9), 879−884.
(32) Somoza, J. R., Skene, R. J., Katz, B. A., Mol, C., Ho, J. D., Jennings, A. J., Luong, C., Arvai, A., Buggy, J. J., Chi, E., Tang, J., Sang, B. C., Verner, E., Wynands, R., Leahy, E. M., Dougan, D. R., Snell, G., Navre, M., Knuth, M. W., Swanson, R. V., McRee, D. E., and Tari, L. W. (2004) Structural snapshots of human HDAC8 provide insights into the class I histone deacetylases. *Structure 12* (7), 1325−34.
(33) Decroos, C., Clausen, D. J., Haines, B. E., Wiest, O., Williams, R. M., and Christianson, D. W. (2015) Variable Active Site Loop Conformations Accommodate the Binding of Macrocyclic Largazole Analogues to HDAC8. *Biochemistry 54* (12), 2126−35.
(34) Vannini, A., Volpari, C., Filocamo, G., Casavola, E. C., Brunetti, M., Renzoni, D., Chakravarty, P., Paolini, C., De Francesco, R., Gallinari, P., Steinkuhler, C., and Di Marco, S. (2004) Crystal structure of a eukaryotic zinc-dependent histone deacetylase, human HDAC8, complexed with a hydroxamic acid inhibitor. *Proc. Natl. Acad. Sci. U. S. A. 101* (42), 15064−9.
(35) Cole, K. E., Dowling, D. P., Boone, M. A., Phillips, A. J., and Christianson, D. W. (2011) Structural basis of the antiproliferative activity of largazole, a depsipeptide inhibitor of the histone deacetylases. *J. Am. Chem. Soc. 133* (32), 12474−7.
(36) Kim, B., Pitcairn, C. A., Lopez, J. E., and Fierke, C. A. (2017) Second Shell Residues Modulate the Reactivity and Metal Selectivity of Histone Deacetylase 8. Manuscript in preparation.
(37) Kim, A. M., Vogt, S., O'Halloran, T. V., and Woodruff, T. K. (2010) Zinc availability regulates exit from meiosis in maturing mammalian oocytes. *Nat. Chem. Biol. 6* (9), 674−81.
(38) Kim, A. M., Bernhardt, M. L., Kong, B. Y., Ahn, R. W., Vogt, S., Woodruff, T. K., and O'Halloran, T. V. (2011) Zinc sparks are triggered by fertilization and facilitate cell cycle resumption in mammalian eggs. *ACS Chem. Biol. 6* (7), 716−23.
(39) Maret, W., and Krężel, A. (2007) Cellular Zinc and Redox Buffering Capacity of Metallothionein/Thionein in Health and Disease. *Mol. Med. 13* (7−8), 371−375.
(40) Kröncke, K.-D. (2007) Cellular stress and intracellular zinc dyshomeostasis. *Arch. Biochem. Biophys. 463* (2), 183−187.
(41) Maret, W. (2006) Zinc coordination environments in proteins as redox sensors and signal transducers. *Antioxid. Redox Signaling 8* (9−10), 1419−1441.
(42) Marschner, A., and Klein, C. D. (2015) Metal promiscuity and metal-dependent substrate preferences of Trypanosoma brucei methionine aminopeptidase 1. *Biochimie 115*, 35−43.
(43) Huguet, F., Melet, A., Alves de Sousa, R., Lieutaud, A., Chevalier, J., Maigre, L., Deschamps, P., Tomas, A., Leulliot, N., Pages, J. M., and Artaud, I. (2012) Hydroxamic acids as potent inhibitors of Fe(II) and Mn(II) E. coli methionine aminopeptidase: biological activities and X-ray structures of oxazole hydroxamate-EcMetAP-Mn complexes. *ChemMedChem 7* (6), 1020−30.

DOI: 10.1021/acs.biochem.7b00851
Biochemistry 2017, 56, 5663−5670

(44) Dai, Y., Wensink, P. C., and Abeles, R. H. (1999) One Protein, Two Enzymes. *J. Biol. Chem. 274* (3), 1193−1195.
(45) Gattis, S. G., Hernick, M., and Fierke, C. A. (2010) Active Site Metal Ion in UDP-3-O-((R)-3-Hydroxymyristoyl)-N-acetylglucosamine Deacetylase (LpxC) Switches between Fe(II) and Zn(II) Depending on Cellular Conditions. *J. Biol. Chem. 285* (44), 33788−33796.
(46) Kim, B., Pithadia, A. S., and Fierke, C. A. (2015) Kinetics and Thermodynamics of Metal-binding to Histone Deacetylase 8. *Protein Sci. 24* (3), 354−365.
(47) Suzuki, T., Ota, Y., Ri, M., Bando, M., Gotoh, A., Itoh, Y., Tsumoto, H., Tatum, P. R., Mizukami, T., Nakagawa, H., Iida, S., Ueda, R., Shirahige, K., and Miyata, N. (2012) Rapid Discovery of Highly Potent and Selective Inhibitors of Histone Deacetylase 8 Using Click Chemistry to Generate Candidate Libraries. *J. Med. Chem. 55* (22), 9562−9575.
(48) Suzuki, T., Muto, N., Bando, M., Itoh, Y., Masaki, A., Ri, M., Ota, Y., Nakagawa, H., Iida, S., Shirahige, K., and Miyata, N. (2014) Design, Synthesis, and Biological Activity of NCC149 Derivatives as Histone Deacetylase 8-Selective Inhibitors. *ChemMedChem 9* (3), 657−664.

DOI: 10.1021/acs.biochem.7b00851
Biochemistry 2017, 56, 5663−5670